Journal of Neuroscience Methods, 46 (1993) 159–166

NSM 01457

Reduced compartmental models of neocortical pyramidal cells

Paul C. Bush and Terrence J. Sejnowski

Howard Hughes Medical Institute and Computational Neurobiology Laboratory, Salk Institute, La Jolla, CA 92037 and University of California at San Diego, La Jolla, CA 92033 (USA)

(Received 20 April 1992, revised version received 29 October 1992, accepted 9 November 1992)

Key words: Neocortex; Pyramidal cell; Computer simulation; Compartmental model

Model neurons composed of hundreds of compartments are currently used for studying phenomena at the level of the single cell. Large network simulations require a simplified model of a single neuron that retains the electrotonic and synaptic integrative properties of the real cell. We introduce a method for reducing the number of compartments of neocortical pyramidal neuron models (from 400 to 8–9 compartments) through a simple collapsing method based on conserving the axial resistance rather than on the surface area of the dendritic tree. The reduced models retain the general morphology of the pyramidal cells on which they are based, allowing accurate positioning of synaptic inputs and ionic conductances on individual model cells, as well as construction of spatially accurate network models. The reduced models run significantly faster than the full models, yet faithfully reproduce their electrical responses.

Introduction

Compartmental computer models have been used to investigate many aspects of single neurons, including passive properties (Rall, 1964; Shelton, 1985), the role of active conductances in producing observed firing behavior (Yamada et al., 1989; Bush and Sejnowski, 1991), and synaptic integration (Rall, 1967; Shepherd et al., 1985; Fleshman et al., 1988; Clements and Redman, 1989; Bernander et al., 1991; Lytton and Sejnowski, 1991; Segev et al., 1992; Bush and Sejnowski, 1992). The models used in these studies contain hundreds of compartments and thousands of coupled differential equations must be solved each time step. To speed up simulations, model networks use simplified representations of the single neurons that comprise the network.

Correspondence: Paul Bush, Computational Neurobiology Laboratory, Salk Institute for Biological Studies, P.O. Box 85800, San Diego, CA 92186-5800, USA. Tel.: (619) 453-4100, ext. 374; FAX: (619) 587-0417; e-mail: paul@helmholtz.sdsc.edu.

Most model neurons composed of just a few compartments have been assigned a somewhat arbitrary geometry, with no systematic testing of the reduced model against the real cell or a more complete model (Traub, 1982; Wehmeier et al., 1989; Wilson and Bower, 1989; Lytton and Sejnowski, 1991). Such models may have the same input resistance (R_{in}) and membrane time constant (τ_m) as the real cell, but typically will not accurately simulate the integration of synaptic inputs in the dendritic compartments and the resulting flow of current into the soma. Recent experimental and theoretical evidence indicates that the electrotonic structure of cortical neurons causes significant non-linearities in the integration of synaptic input (Ferster and Jagadeesh, 1991; Bush and Sejnowski, 1992; Ferster and Jagadeesh 1992). It is still an open question as to whether such effects are important at the level of network function, but it would be prudent to ensure that a simplified model neuron destined for network simulation is an as accurate representation of the real cell as possible.

An example of a simplified model neuron that does retain the electrotonic characteristics of the

full model is the 'cartoon representation' developed by Stratford et al. (1989). This is a model of a cortical pyramidal cell reduced to 24 compartments by using a number of mathematical transformations to collapse the basal and apical dendritic trees into equivalent profiles, then collapsing all the oblique dendrites (lateral branches from the apical trunk) that are at the same electrotonic distance from the soma. Stratford et al. (1989) demonstrated that the cartoon model is a good fit to the full model in terms of its response to transient current injections at different locations as well as displaying the same R_{in} and τ_m. We have combined this approach with a simpler method to construct an alternative cartoon representation that allowed us to achieve fewer compartments yet retain accurate electrical properties..

Methods

Simulations were performed using standard techniques for compartmental models of branching dendritic trees (Rall, 1964); 2 digitized HRP-filled pyramidal cells from cat visual cortex (layers 2 and 5) (Koch et al., 1990) were modeled, each consisting of coupled cylindrical compartments containing only resistive and capacitative elements. The full models against which the reduced models were tested had approximately 400 compartments (Fig. 1A), and have been used in a number of previous studies (Koch et al., 1990; Bernander et al., 1991; Lytton and Sejnowski, 1991; Bush and Sejnowski, 1992). The simulator CABLE (Hines, 1989), running on a MIPS Magnum 3000/33, required about 1 min of computation to simulate 100 ms of real time for the full

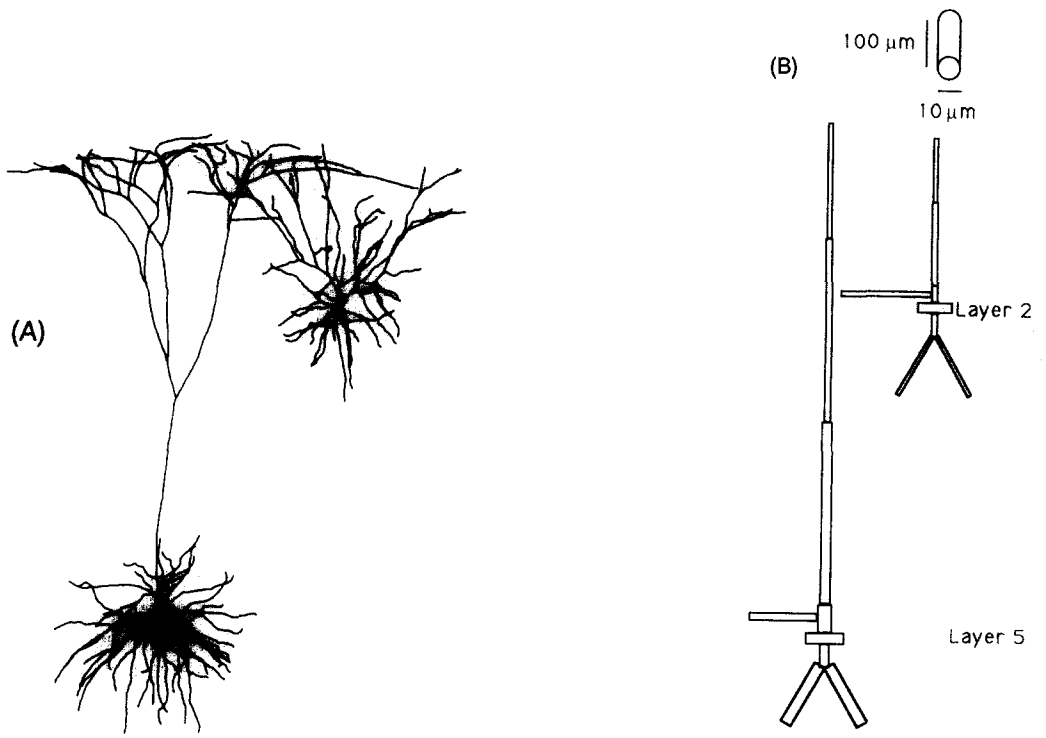

Fig. 1. A: drawings of reconstructed HRP-filled layer 2 (right) and layer 5 (left) pyramidal cells. B: geometries of reduced pyramidal cell models (see Table I for lengths and diameters of each compartment).

models. The reduced models ran approximately 5 times faster in simulations that included a full set of voltage- and ligand-gated conductances.

Model parameters

The choice of values for the passive parameters (specific membrane resistance, R_m; specific membrane capacitance, C_m; and axial resistivity, R_i) for pyramidal cells has recently been discussed (Bush and Sejnowski, 1992). Following that study, we used $C_m = 1\ \mu F/cm^2$ (Jack et al., 1975), $R_i = 200\ \Omega cm$ (Shelton, 1985; Stratford et al., 1989; Bernander et al., 1991; Segev et al., 1992) and $R_m = 20\ 000\ \Omega cm^2$. This value for R_m is the effective specific membrane resistance for an in vivo neocortical pyramidal neuron receiving background synaptic input from spontaneously active neurons (Barrett and Crill, 1974; Bernander et al., 1991). These passive parameters produced R_{in}s for the model layer-5 and layer-2 pyramidal cells of 45 MΩ and 110 MΩ, respectively, and a τ_m of 20 ms. These values are within the range recorded from cells in cat visual cortex in vivo (Douglas et al., 1991; Pei et al., 1991; Ferster and Jagadeesh, 1992).

The inclusion of spines in a passive model may significantly increase the membrane area of the cell (Stratford et al., 1989; Segev et al., 1992). A recent calculation has shown that the addition of the membrane area of 4000 spines to our layer-5 pyramidal cell increases the area by about 7.5% (Bernander et al., 1992). This can be accounted for in a model by increasing C_m and proportionally decreasing R_m (Holmes, 1989). Our values for R_m and C_m are constrained by measurements of R_{in} and τ_m and are not based on direct measurement. Thus, if we assume that adding spines increases the membrane area of our pyramidal cells by 20%, for example, we revise our estimate of R_m to 24 kΩcm^2 and our estimate of C_m to 0.8 $\mu F/cm^2$. These values are then decreased and increased, respectively, to account for spine membrane, producing the values that we use in our model. We have found very little difference between results obtained with excitatory synaptic inputs on the heads of explicitly modeled spines as opposed to those obtained with inputs made directly onto dendritic shafts (Bush and Sejnowski, 1992). Thus, in these simulations synaptic inputs were made directly onto dendritic shafts.

Excitatory (EPSP) and inhibitory (IPSP) postsynaptic potentials in our models were simulated as alpha function conductance changes with a peak amplitude of 0.5 nS and a time to peak of 1 ms (Rall, 1967; Bernander et al., 1991). These parameters were chosen because they produced EPSPs at the soma with the same time course and amplitude as those observed experimentally (Thomson et al., 1988; Mason et al., 1991). The reversal potential for EPSPs was 0 mV and the reversal potential for IPSPs was -70 mV (Connors et al., 1988; McCormick, 1989). Trains of EPSPs or IPSPs were modeled according to a Poisson distribution with a fixed mean frequency of activation.

For some simulations, active conductances were placed at the soma to generate adapting trains of action potentials, as observed in regular-firing cortical neurons (McCormick et al., 1985). The conductances followed Hodgkin-Huxley-like kinetics based on parameters developed by Borg-Graham (1987). The implementation was exactly as described in Bush and Sejnowski (1992).

Reduced compartmental models

When reducing a compartmental model to one with fewer compartments, R_m, $C_m$and R_i should be preserved so that the reduced model will have the same R_{in}, τ_m and length constant (l) as the full model. Pyramidal cells do not obey Rall's constraints for collapse into a single equivalent cylinder (Stratford et al., 1989; Douglas and Martin, 1991), so other approaches must be tried. Surface area (hence R_m and C_m) can be conserved by constructing an 'equivalent dendritic profile' (Fleshman et al., 1988; Clements and Redman, 1989; Stratford et al., 1989; Manor et al., 1991). In this technique the sum of the diameters to the 3/2 power of all the dendrites at regular intervals from the soma are used to compute the diameter of an equivalent dendrite. The length of the equivalent dendrite must also be scaled appropriately. As shown by Stratford et al. (1989), the equivalent profile has the same R_{in} and τ_m as the full model but the degree of attenuation of synaptic input along the length of

the apical dendrite is not large enough. This is because the axial resistance of the equivalent profile is not equal to the axial resistance of the apical dendrite, due to the lumping of the oblique dendrites into the profile. The cartoon model developed by Stratford et al. (1989) solved this problem by explicitly representing the oblique dendrites as sidebranches from the apical trunk.

An alternative approach to the cartoon representation is a collapsing technique based on conserving R_i rather than the membrane surface area. This is done by making the cross-sectional area of the equivalent cylinder equal to the sum of the cross-sectional areas of all the dendrites represented by that equivalent cylinder:

$$R = \sqrt{\sum_i r_i^2} \qquad (1)$$

where R is the radius of the equivalent cylinder and r_i is the radius of dendrite i. The length of the equivalent cylinder is just the average length of all the dendrites represented by the equivalent cylinder.

We have applied this collapsing technique to create a new reduced pyramidal cell model. First, all dendrites with approximately the same origin and (electrotonic) length are collapsed into a single equivalent cable. Thus, all the preterminal basal dendritic segments (Larkman, 1991a) were collapsed together into an equivalent cylinder, as were all the terminal basal dendritic segments. The distal apical dendritic aborization was also collapsed together. The main apical dendrite was reduced to 2 or 3 equivalent cylinders. To insure the correct attenuation along the apical dendrite, the oblique dendrites were represented as a single sidebranch from the apical trunk. Some fine tuning of the structure obtained using this method was required; in particular we found it necessary to use two paired basal dendritic compartments rather than one. This was to ensure a large enough dendritic load on the soma while maintaining the correct attenuation from dendrites to soma: a single large-diameter cylinder does not show great enough attenuation of synaptic input. The somatic compartment had the same dimensions as in the full model.

TABLE I

DIMENSIONS OF REDUCED MODELS

	Layer 5 pyramid		Layer 2 pyramid	
	Length (μm)	Diameters (μm)	Length (μm)	Diameters (μm)
Soma	23	17	21	15.3
Apical trunk	60	6	35	2.5
Obliques	150	3	200	2.3
Apical no. 1	400	4.4	180	2.4
Apical no. 2	400	2.9	–	–
Apical tuft	250	2	140	2
Basal trunk	50	4	50	2.5
Basals (2)	150	5	150	1.6

The surface areas of our reduced models are less than those of the full models. Thus the next step in the reduction was to scale the values used for R_m and C_m appropriately. R_i was conserved, so R_m could be changed until the reduced model had the same R_{in} as the full model. We found that R_m had to be reduced by 2.84 times to match the R_{in} of the reduced layer 5-cell model with that of the full layer 5-cell model. R_m had to be reduced by 2.95 times to match the R_{in} of the reduced layer 2-cell model with that of its full model. C_m must then be multiplied by this scaling factor to match τ_m of the reduced cell to that of the full cell. This procedure is a correction for the reduction in surface area, and indeed if an approximate calculation of the ratio of the areas of the full and reduced layer 5-cell model is made by summing up the areas of all the cylindrical compartments in each model, a value of 2.74 is obtained, which is quite close to the empirical scaling factor of 2.84. The dimensions of the reduced models are given in Table I.

Our collapsing method is simpler than that of Stratford et al. (1989) and allowed us to produce accurate models composed of less than 10 compartments. In addition, the lengths of our equivalent dendrites were equal to the average lengths of the dendrites which they represent. This is important when incorporating these models into spatially accurate networks.

Our method takes advantage of some of the morphological features of neocortical pyramidal cells: all the dendrites collapsed together into an equivalent cylinder have approximately equal

lengths and diameters, as well as equivalent electrotonic origins. It should be possible to construct similar models of other types of neurons using our method if their dendritic morphologies display these features.

Results

The geometries of the reduced model layer-2 and layer-5 pyramidal cells are shown in Fig. 1B. Drawings of the HRP-filled pyramidal cells are included for comparison (Fig. 1A). In order to assess the accuracy of the method that produced the reduced models, we compared the responses of the reduced and full models to different types of stimulation. The response of the reduced and the full model layer-5 pyramid to a continuous somatic current injection of -0.7 nA are compared in Fig. 2A. The superposition of the two traces shows that both models have the same R_{in} and τ_m. It is relatively easy to match these parameters by tuning R_m and C_m. Such a match says little about how faithfully the reduced model captures the synaptic integration properties of the full model (Fleshman et al., 1988). The responses of the reduced and the full model layer-2 pyramid to a brief somatic current injection are compared in Fig. 2B (Shelton, 1985; Stratford et al., 1989). The response to a transient somatic input is dependent on R_i as well as R_m and C_m, because it is dependent on how fast current moves from the soma into the dendrites. The response of the reduced model is a good fit to that of the full model. The responses of both models to an EPSP on the soma, with 0.5 nS peak conductance are compared in Fig. 2C. This tests essentially the same properties as the brief current pulse; the

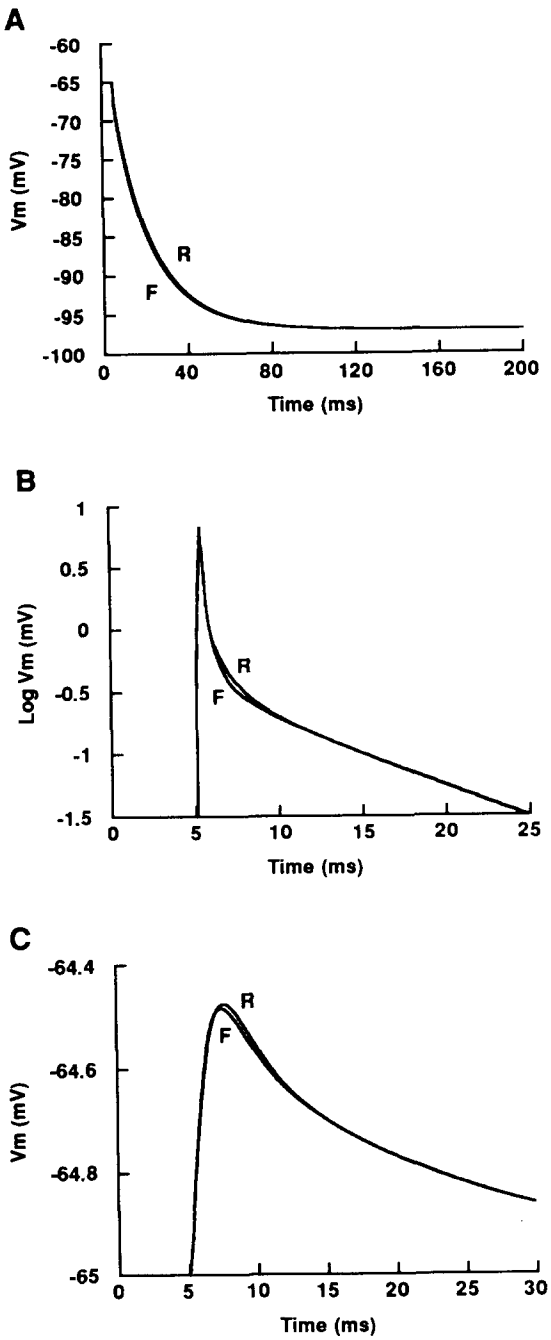

Fig. 2. Comparison of the response of the reduced (R) and full (F) models to somatic input. A: voltage response at the soma of reduced and full layer 5 pyramid models to constant current injection of -0.7 nA. The superposition of the two traces indicates that both models have the same R_{in} and τ_m. B: semi-log plot of voltage response of reduced and full layer 2 models to a 0.44 ms 0.3 nA somatic current injection at t = 5 ms. C: voltage response of both layer 2 models to a 0.5 nS somatic EPSP. The close fit of the reduced model with the full model to these transient inputs indicates that the dendrites conduct charge away from the soma at the same rate in both models.

performance of the reduced model is very close to that of the full model.

Fig. 3A shows the firing of the full 400 compartment layer-5 cell in response to a maintained 1 nA somatic current injection. The model cell produced an adapting spike train typical of the regular-firing class of cortical pyramidal cells (McCormick et al., 1985). The conductances underlying this firing behavior, located in the soma only, were put into the 9-compartment model without changing a single parameter. Because both models have the same somatic dimensions, the same conductance densities were used in both. Fig. 3B shows the firing of the 9-compartment model in response to a 1 nA somatic current injection. The response of the reduced model has the same form as that of the full model – an adapting train of action potentials. The firing frequency of the reduced model was slightly higher, but the small difference was within the limits of uncertainty of the model parameters as well as the variance in response recorded across different pyramidal cells (McCormick et al., 1985; Douglas et al., 1991).

The final test was to compare the response of both models to synaptic input. To produce the same output as the full model, the reduced model must perform the same non-linear integration of dendritic EPSPs and IPSPs as the full model (Bush and Sejnowski, 1992), and display the same dendrites-to-soma transfer characteristics. In other words, the reduced model must have the same input-output function as the full model.

A majority (70–90%) of excitatory inputs to cortical pyramidal cells are made on the basal/oblique dendrites (Larkman, 1991b). We

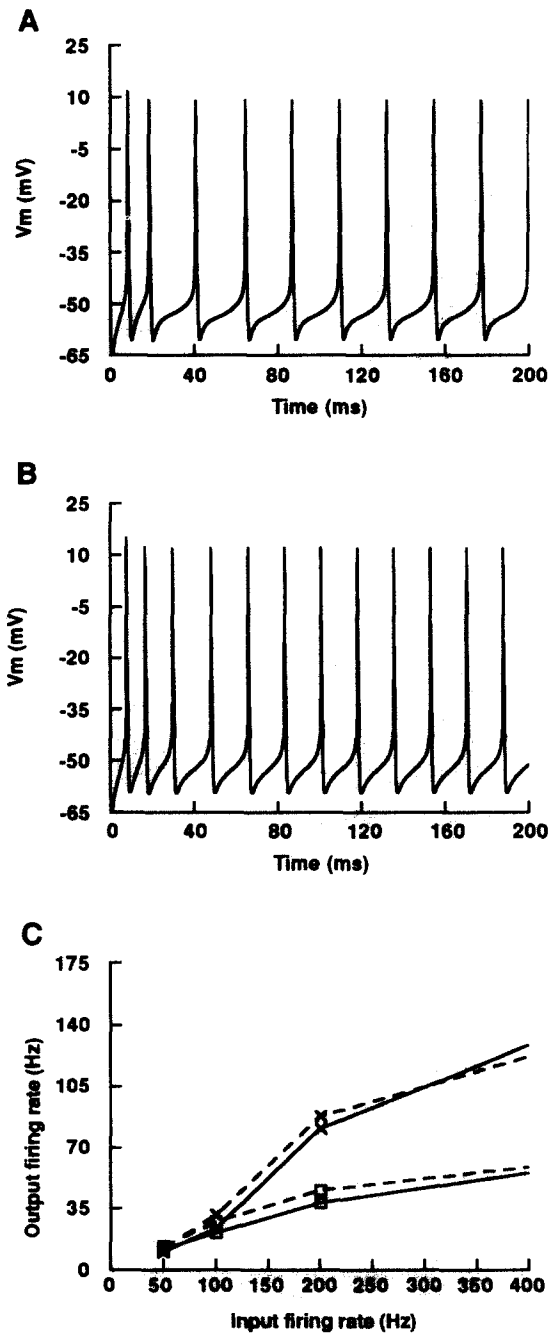

Fig. 3. Comparison of firing responses of reduced and full model layer 5 pyramidal cell. The somata of both models contain active conductances with exactly the same kinetics and densities. A: adapting spike train of full model in response to constant 1 nA somatic current pulse. B: spike train of reduced model in response to same stimulus. The response of the reduced model is of the same form as that of the full cell, but the firing frequency is slightly higher. C: firing rate of full (solid traces) and reduced (dashed traces) models as a function of the firing rate of their 140 excitatory inputs. Each model also receives 45 inhibitory synapses, active at twice the rate of the excitatory ones. X = initial, peak firing rate. □ = steady, adapted firing rate. The close fit of the two models demonstrates that the reduced model integrates excitatory and inhibitory synaptic input in the same manner as the full model.

distributed synapses on the dendrites and soma to reflect these measurements. Thus, 140 excitatory synapses were placed randomly on the basal and oblique dendrites of the full model and 140 on the 1 oblique and 2 basal equivalent dendrites of the reduced model. In addition, 33 inhibitory synapses were placed on the proximal dendrites and 12 on the soma of each model, a pattern of innervation characteristic of basket cells, the most common inhibitory cell type in cortex (Martin, 1988). Inhibitory (smooth) cells fire at much higher rates than pyramidal cells (McCormick et al., 1985), therefore inhibitory synapses were activated at a mean frequency twice that of the excitatory synapses. Fig. 3C shows the responses of the full and reduced models for the peak (initial) and steady-state (adapted) firing rates as a function of the frequency of the excitatory inputs. The fit is close for all input frequencies, demonstrating that the reduced model shows about the same dendritic integration characteristics and response to inhibition as the full model, despite having an extremely simplified structure.

Discussion

Given current computational limitations, simulation of a large, realistic network requires a model cell with a minimal number of compartments. The reduced pyramidal cell model presented here is a good fit to the full model for a variety of stimuli (Figs. 2 and 3), and is suitable for network simulations involving multiple, spatially separated synaptic inputs to the neurons.

The R_{in} of an equivalent dendrite of the reduced model is not as large as the R_{in} of one of the dendrites represented by the equivalent dendrite. Hence, a single EPSP on an equivalent dendrite of the reduced model is not equivalent to a single EPSP on a single dendrite of the full model. Rather it would be equivalent to dividing the EPSP and applying one fraction to each of the real dendrites represented by the equivalent dendrite. Thus, the reduced model is not appropriate for studying the effect of single synaptic inputs on single dendritic branches of pyramidal cells or local dendritic processing in general. For example, we would not use this reduced model to investigate clustering of individual synaptic inputs or the inhibitory control of specific dendrites. Such studies must use more detailed models that represent each process of the neuron explicitly. However, we found that the membrane potential of the basal dendrites of the reduced model was equal to the mean potential of the basal dendrites of the full model during multiple synaptic activation (e.g., Fig. 3C), giving us some confidence that the voltage-dependent processes (such as NMDA) occurring in the dendrites (as well as the soma) during multiple synaptic activation could be accurately simulated with the reduced model.

Acknowledgements

We thank R.J. Douglas and K.A.C. Martin for providing us with the cortical cell morphologies.

References

Barrett, J.N. and Crill, W.E. (1974) Influence of dendritic location and membrane properties on the effectiveness of synapses on cat motoneurones. J. Physiol., 293: 325–345.

Bernander, O., Douglas, R.J., Martin, K.A.C. and Koch, C. (1991) Synaptic background activity influences spatiotemporal integration in single pyramidal cells. Proc. Natl. Acad. Sci., 88: 11569–11573.

Bernander, O., Douglas, R.J. and Koch, C. (1992) A model of regular-firing cortical pyramidal neurons (16). California Institute of Technology.

Borg-Graham, L.J. (1987) Modeling the somatic electrical response of hippocampal pyramidal neurons. MIT.

Bush, P.C. and Sejnowski, T.J. (1991) Simulations of a reconstructed cerebellar purkinje cell based on simplified channel kinetics. Neural Comp., 3: 299–309.

Bush, P.C. and Sejnowski, T.J. (1992) Dendritic saturation and effects of inhibition in simulated neocortical pyramidal cells. J. Neurophysiol., submitted for publication.

Clements, J.D. and Redman, S.J. (1989) Cable properties a of cat spinal motoneurons measured by combining voltage clamp, current clamp and intracellular staining. J. Physiol., 409: 63–87.

Connors, B.W., Malenka, R.C. and Silva, L.R. (1988) Two inhibitory postsynaptic potentials, and GABAa and GABAb receptor-mediated responses in neocortex of rat and cat. J. Physiol., 406: 443–468.

Douglas, R.J. and Martin, K.A.C. (1991) A functional microcircuit for cat visual cortex. J. Physiol., 440: 735–769.

Douglas, R.J., Martin, K.A.C. and Whitteridge, D. (1991) An intracellular analysis of the visual responses of neurones in cat visual cortex. J. Physiol., 440: 659–696.

Ferster, D. and Jagadeesh, B. (1991) An in vivo whole-cell patch study of the linearity of IPSP-EPSP interactions in cat visual cortex. Soc. Neurosci. Abst., 17: 176.

Ferster, D. and Jagadeesh, B. (1992) EPSP-IPSP interactions in cat visual cortex studied with in vivo whole-cell patch recording. J. Neurosci., 12: 1262–1274.

Fleshman, J.W., Segev, I. and Burke, R.E. (1988) Electrotonic architecture of type-identified alpha-motoneurons in the cat spinal cord. J. Neurophysiol., 60: 60–85.

Hines, M.L. (1989) A program for simulation of nerve equations with branching geometries. Int. J. Biomed. Comp., 24: 55–68.

Holmes, W.R. (1989) The role of dendritic diameters in maximizing the effectiveness of synaptic inputs. Brain Res., 478: 127–137.

Jack, J.J.B., Noble, D. and Tsien, R.W. (1975) Electric Current Flow in Excitable Cells. Oxford University Press, Oxford.

Koch, C., Douglas, R. and Wehmeier, U. (1990) Visibility of synaptically induced conductance changes: theory and simulations of anatomically characterized cortical pyramidal cells. J. Neurosci., 10: 1728–1744.

Larkman, A.U. (1991a) Dendritic morphology of pyramidal neurons of the visual cortex of the rat. I. Branching patterns. J. Comp. Neurol., 306: 307–319.

Larkman, A.U. (1991b) Dendritic morphology of pyramidal neurons of the visual cortex of the rat. III. Spine distributions. J. Comp. Neurol., 306: 332–343.

Lytton, W.W. and Sejnowski, T.J. (1991) Simulations of cortical pyramidal neurons synchronized by inhibitory interneurons. J. Neurophysiol., 66: 1059–1079.

Manor, Y., Gonczarowski, J. and Segev, I. (1991) Propagation of action potentials along complex axonal trees. Model and implementation. Biophys. J., 60: 1411–1423.

Martin, K.A.C. (1988) From single cells to simple circuits in the cerebral cortex. Quart. J. Exp. Physiol., 73: 637–702.

Mason, A., Nicoll, A. and Stratford, K. (1991) Synaptic transmission between individual pyramidal neurons of the rat visual cortex in vitro. J. Neurosci., 11: 72–84.

McCormick, D.A. (1989) GABA as an inhibitory neurotransmitter in human cerebral cortex. J. Neurophysiol., 62: 1018–1027.

McCormick, D.A., Connors, B.W., Lighthall, J.W. and Prince, D.A. (1985) Comparative electrophysiology of pyramidal and sparsely spiny stellate neurons of the neocortex. J. Neurophysiol., 54: 782–806.

Pei, X., Volgushev, M., Vidyasagar, T.R. and Creutzfeldt, O.D. (1991) Whole cell recording and conductance measurements in cat visual cortex in vivo. NeuroReport. 2: 485–488.

Rall, W. (1964) Theoretical significance of dendritic trees for neuronal input-output relations. In: R. Reiss (Ed.), Neural Theory and Modeling, Stanford University Press, Stanford, CA, pp. 73–97.

Rall, W. (1967) Distinguishing theoretical synaptic potentials computed for different soma-dendritic distributions of synaptic input. J. Neurophysiol., 30: 1138–1168.

Segev, I., Rapp, M., Manor, Y. and Yarom, Y. (1992) Analog and digital processing in single nerve cells: dendritic integration and axonal propagation. In: T. McKenna, J. Javis and S.F. Zornetzer (Eds.), Single Neuron Computation, Academic Press, San Diego, CA.

Shelton, D.P. (1985) Membrane resistivity estimated for the Purkinje neuron by means of a passive computer model. Neuroscience, 14: 111–131.

Shepherd, G.M., Brayton, R.K., Miller, J.F., Segev, I., Rinzel, J. and Rall, W. (1985) Signal enhancement in distal cortical dendrites by means of interactions between active dendritic spines. Proc. Natl. Acad. Sci. USA, 82: 2192–2195.

Stratford, K., Mason, A., Larkman, A., Major, G. and Jack, J. (1989) The modelling of pyramidal neurons in the cat visual cortex. In: R. Durbin, C. Miall and G. Mitchison (Eds.), The Computing Neuron, Addison-Wesley, Wokingham, UK.

Thomson, A.M., Girdlestone, D. and West, D.C. (1988) Voltage-dependent currents prolong single-axon postsynaptic potentials in layer III pyramidal neurons in rat neocortical slices. J. Neurophysiol., 60: 1896–1907.

Traub, R.D. (1982) Simulation of intrinsic bursting in CA3 hippocampal neurons. Neuroscience, 7: 1233–1242.

Wehmeier, U., Dong, D., Koch, C. and Van Essen, D. (1989) Modeling the mammalian visual system. In: C. Koch and I. Segev (Eds.), Methods in Neuronal Modeling, MIT Press, Cambridge, MA, pp. 335–359.

Wilson, M.A. and Bower, J.M. (1989) The simulation of large-scale neural networks. In: C. Koch and I. Segev (Eds.), Methods in Neuronal Modeling: From Synapse to Networks, MIT Press, Cambridge, MA, pp. 291–333.

Yamada, W.M., Koch, C. and Adams, P.R. (1989) Multiple channels and calcium dynamics. In: C. Koch and I. Segev (Eds.), Methods in Neuronal Modeling: From Synapse to Networks, MIT Press, Cambridge, MA, pp. 97–133.